Electronic Supplementary Information (ESI)

Prochelator BHAPI Protects Cells against Paraquat-Induced Damage by ROS-Triggered Iron Chelation

Filip Kielar,[a] Marian E. Helsel,[a] Qin Wang,[a] and Katherine J. Franz*[a]

Department of Chemistry, Duke University, 124 Science Dr., Durham, NC 27708, USA

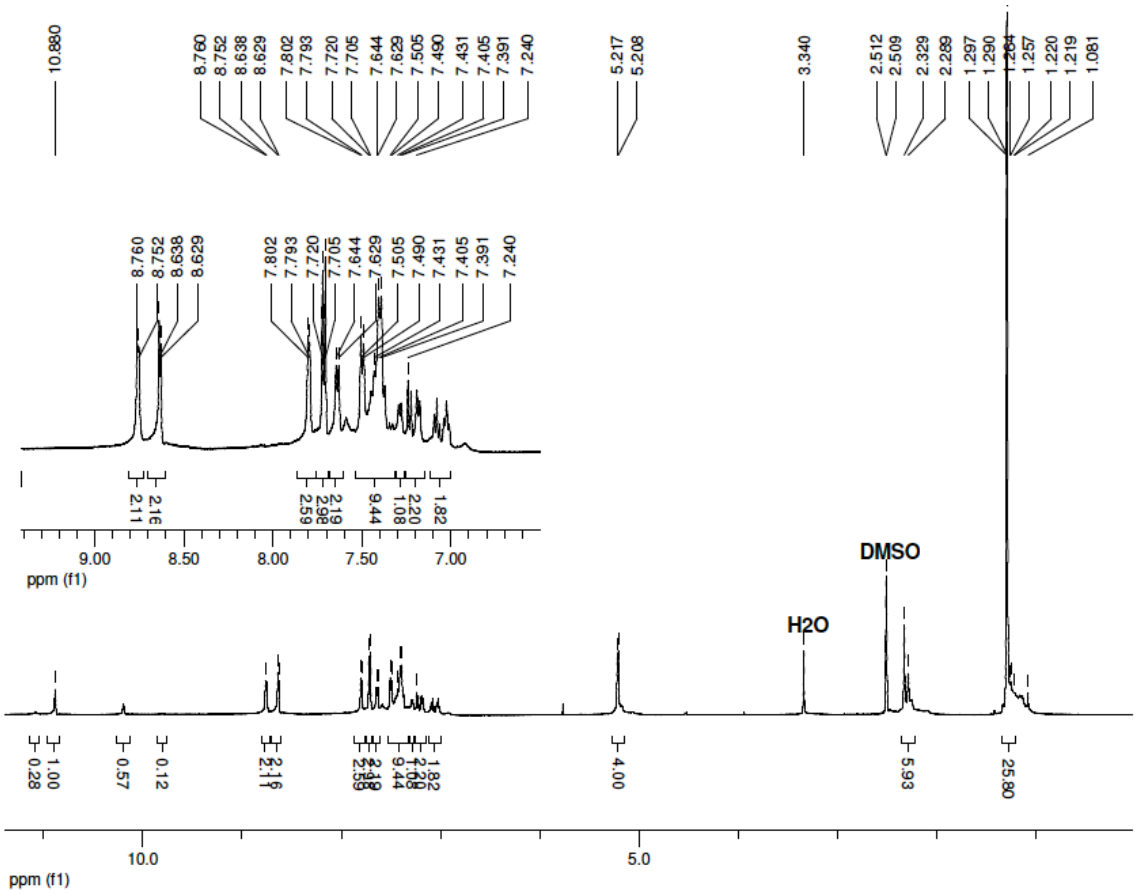

SI Fig. 1 ^{1}H NMR spectrum of BHAPI in d_6-DMSO

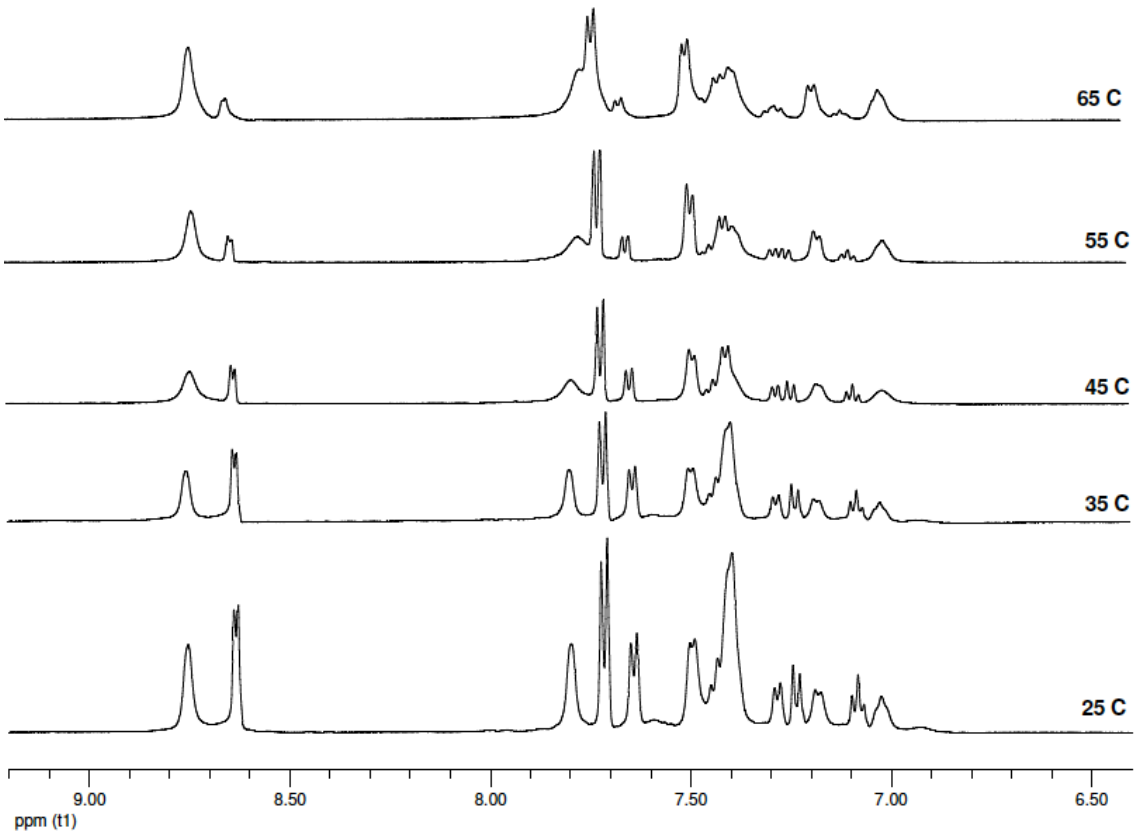

SI Fig. 2 Variable temperature ^{1}H NMR spectra for BHAPI (d_6-DMSO)

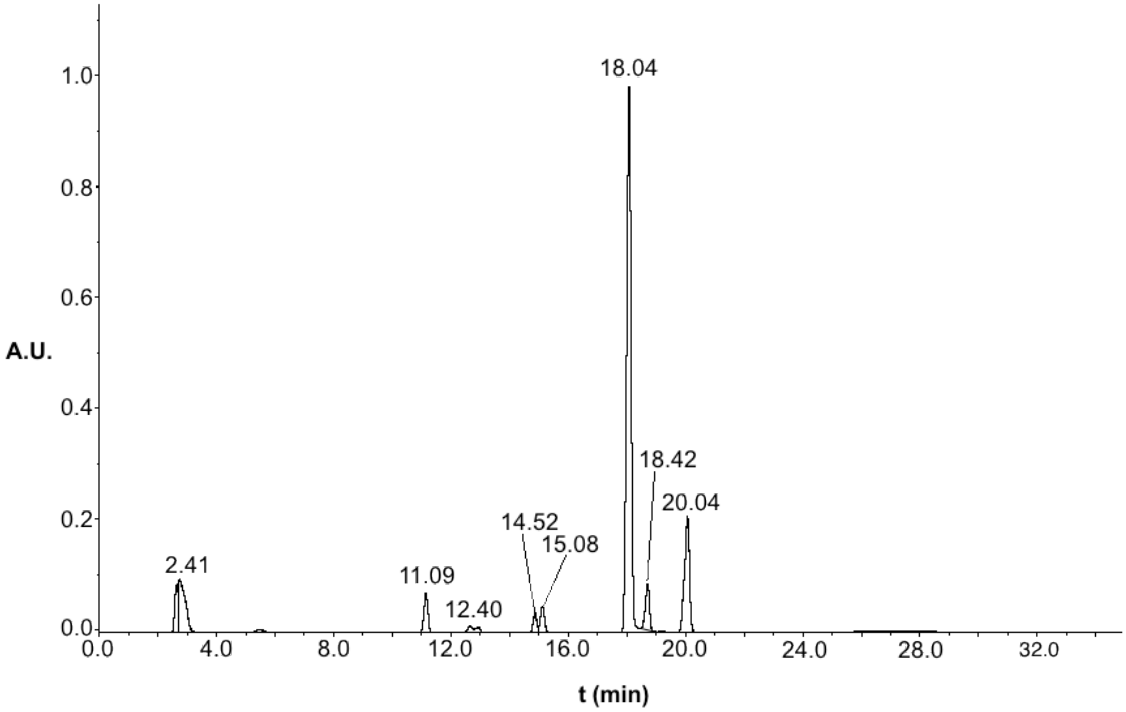

SI Fig . 3 HPLC trace of reaction mixture of BHAPI (1 mM) with hydrogen peroxide (50 mM) in 80% H_2O and 20 % DMSO after 12 h. The labeled peaks were collected for analysis by ^1H NMR and mass spectrometry, see following figures.

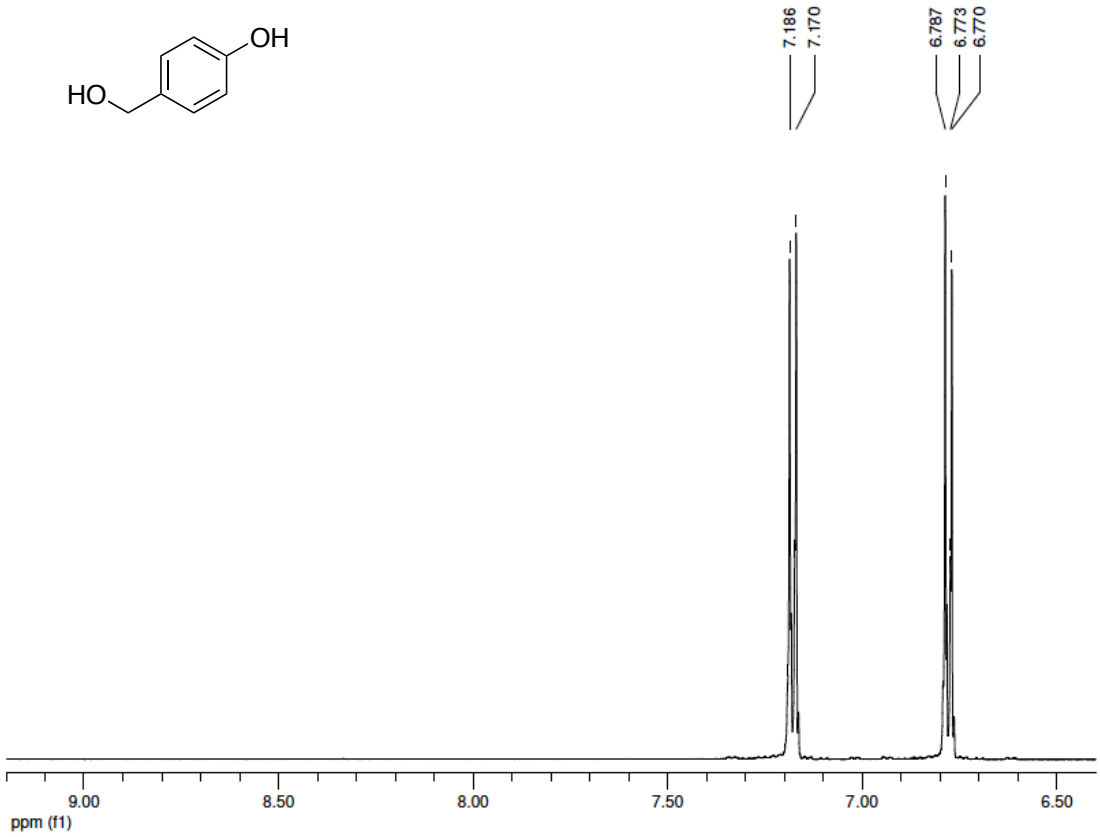

SI Fig. 4 ^{1}H NMR spectrum for compound isolated from peak at 11 min (HPLC trace in SI Fig. 3), which is consistent with the chemical structure shown.

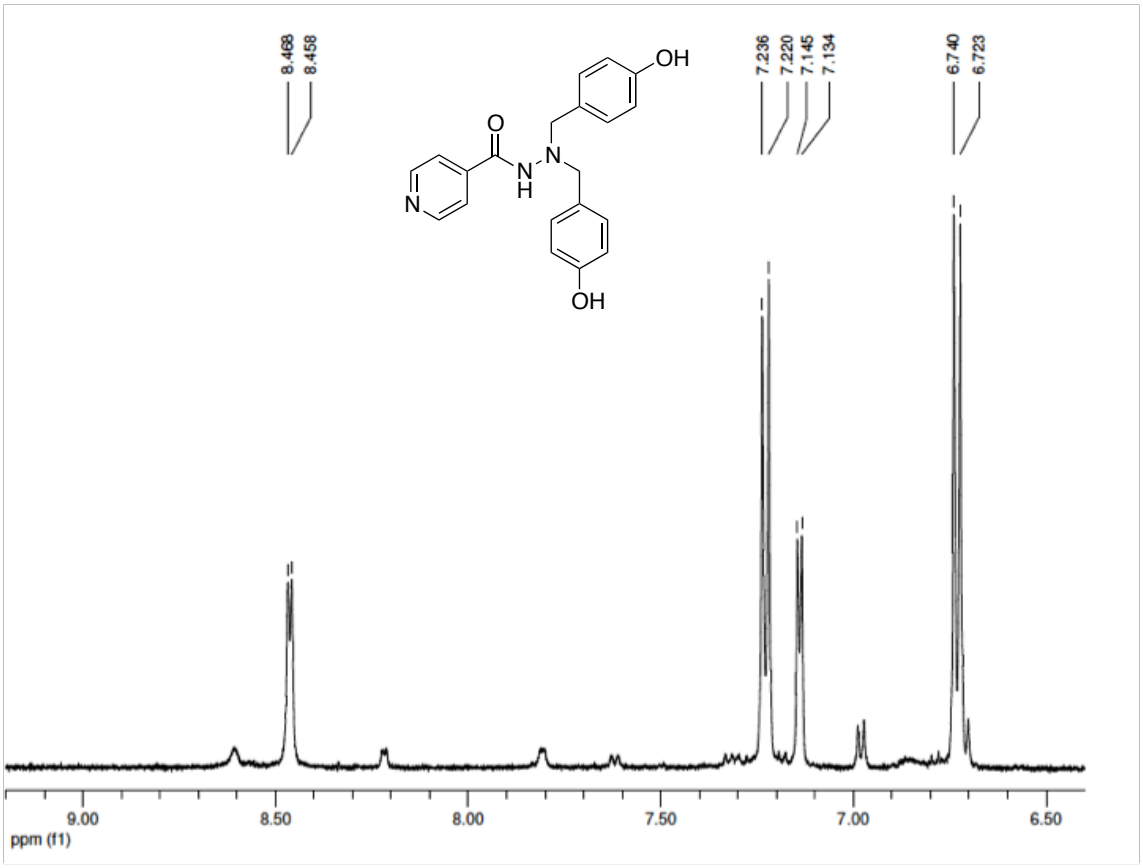

SI Fig. 5 ^{1}H NMR spectrum for compound isolated from peak at 14.5 min (HPLC trace in SI Fig. 3), which is consistent with the chemical structure shown.

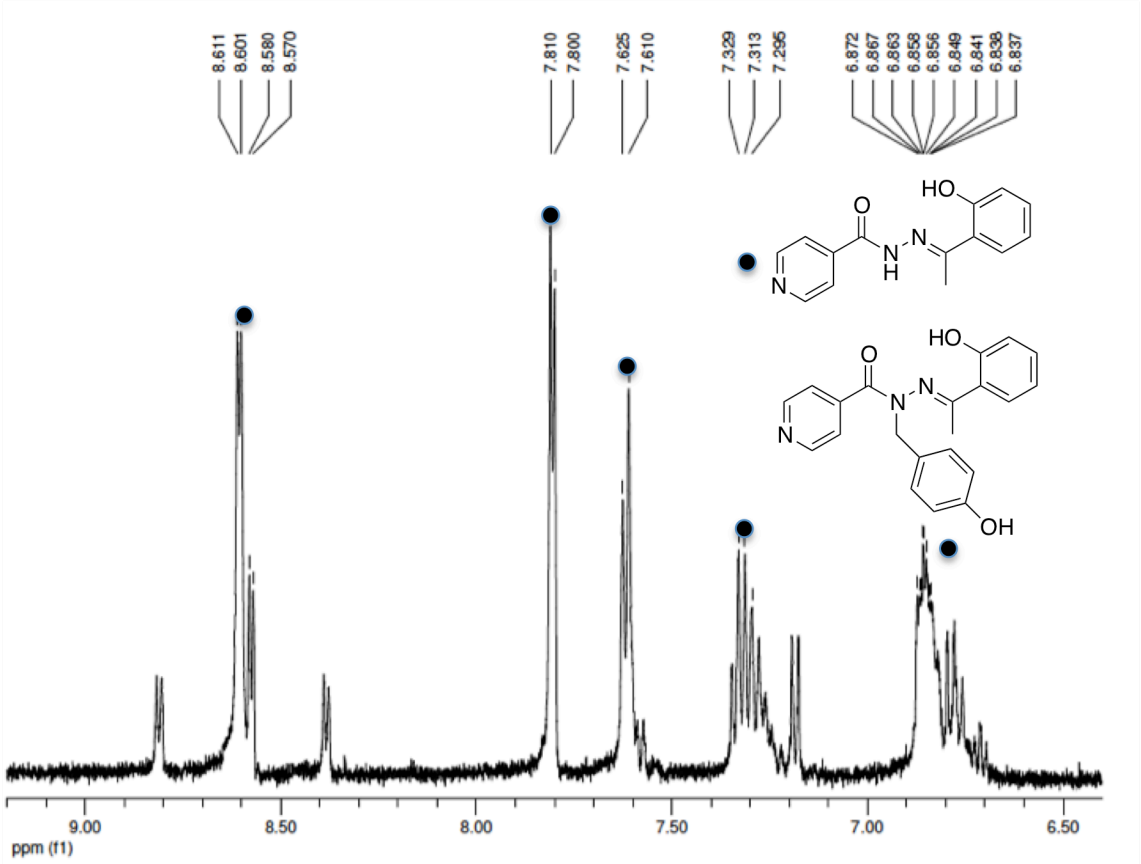

SI Fig. 6 ^{1}H NMR spectrum for compound isolated from peak at 18 min (HPLC trace in SI Fig. 3). HAPI is the main product and peaks belonging to it are designated by black dots. The remaining peaks are consistent with a molecule of structure shown.

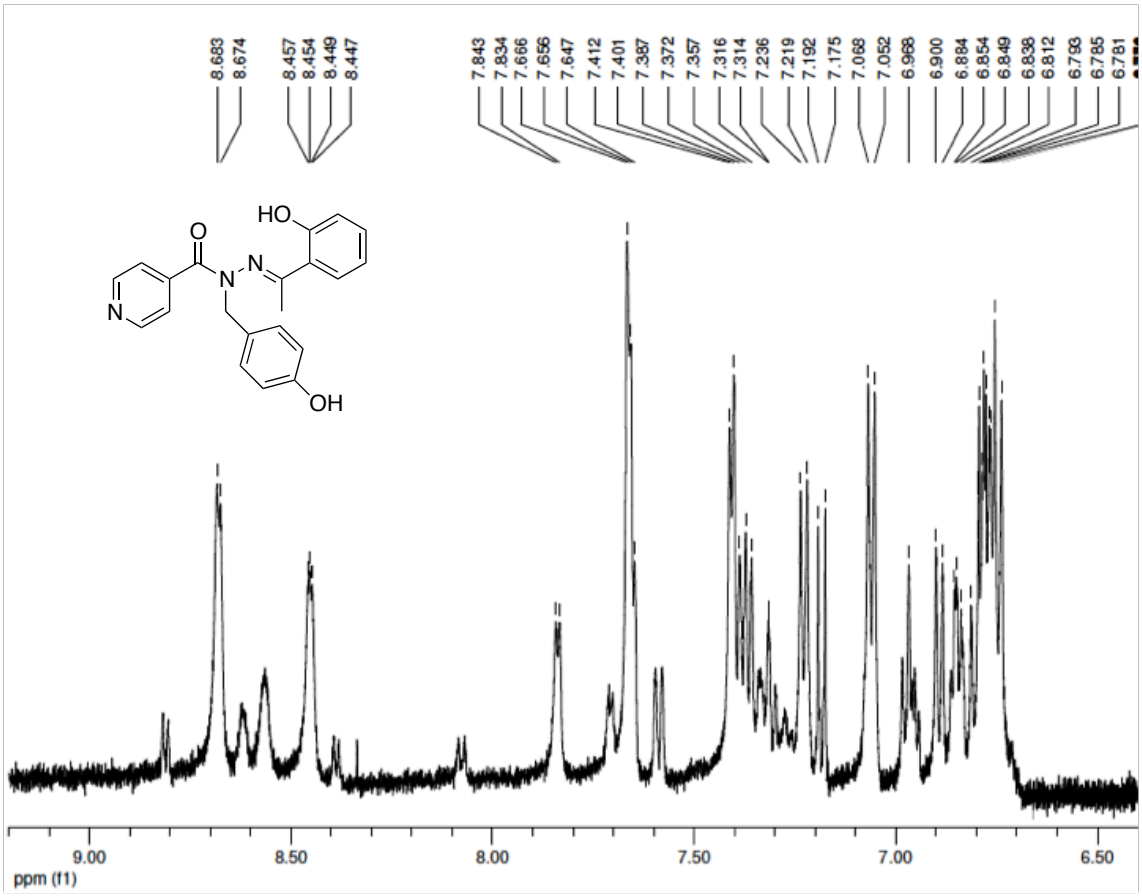

SI Fig. 7 ^{1}H NMR spectrum for product isolated from peak at 18.5 min (HPLC trace in SI Fig. 3). The structure of the proposed sideproduct is based on MS data. This fraction, however contains a more complex mixture of substances.

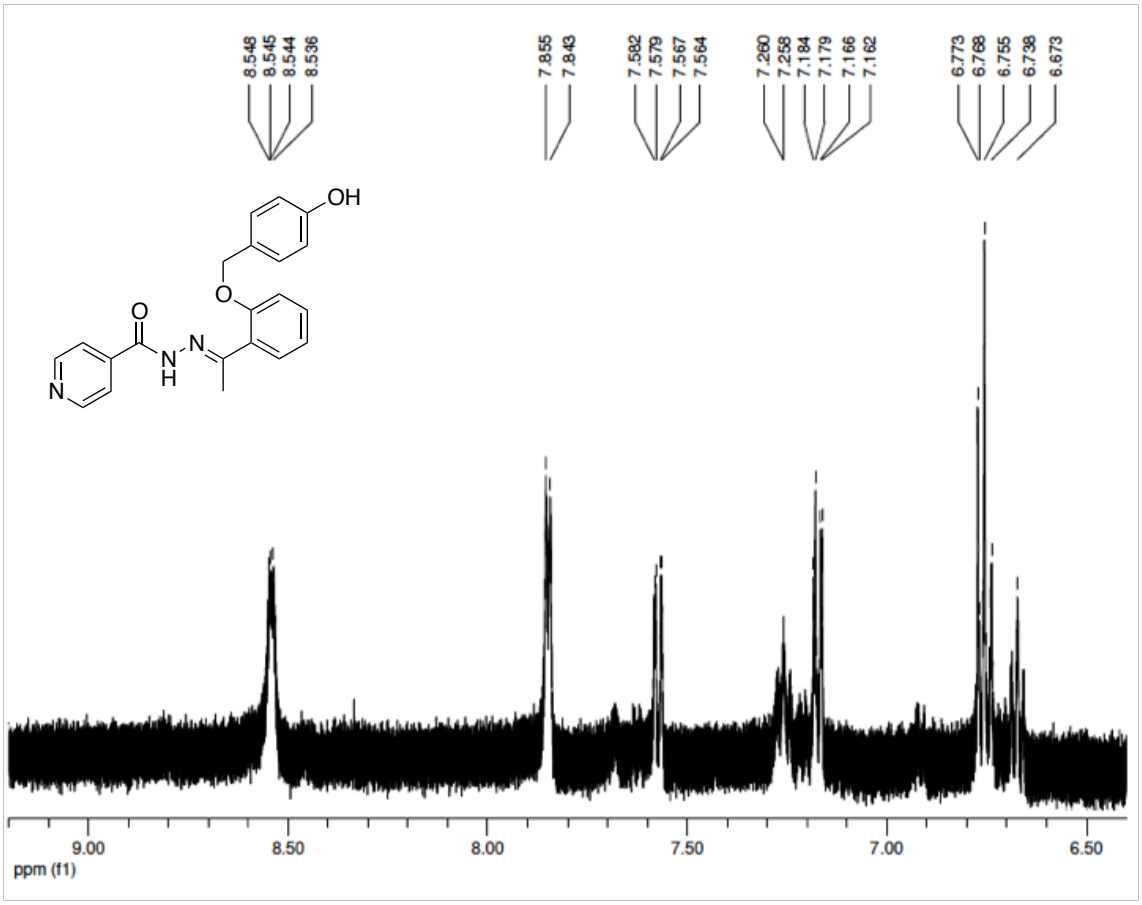

SI Fig. 8 ^{1}H NMR spectrum for compound isolated from peak at 20 min (HPLC trace in SI Fig. 3), which is consistent with the chemical structure shown.

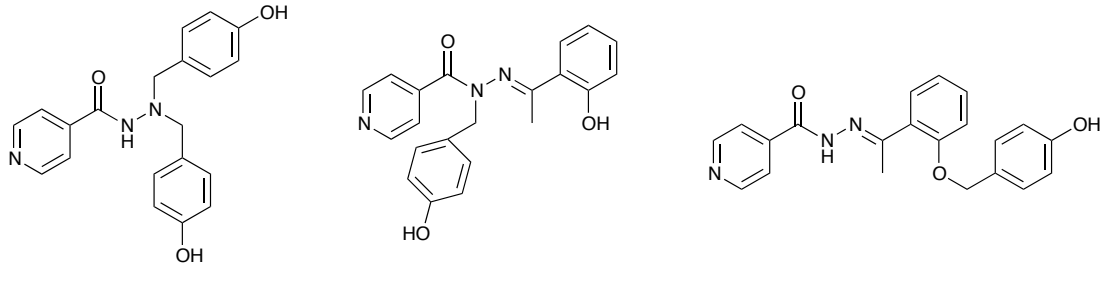

SI Fig. 9 Structures of proposed side products for BHAPI oxidation

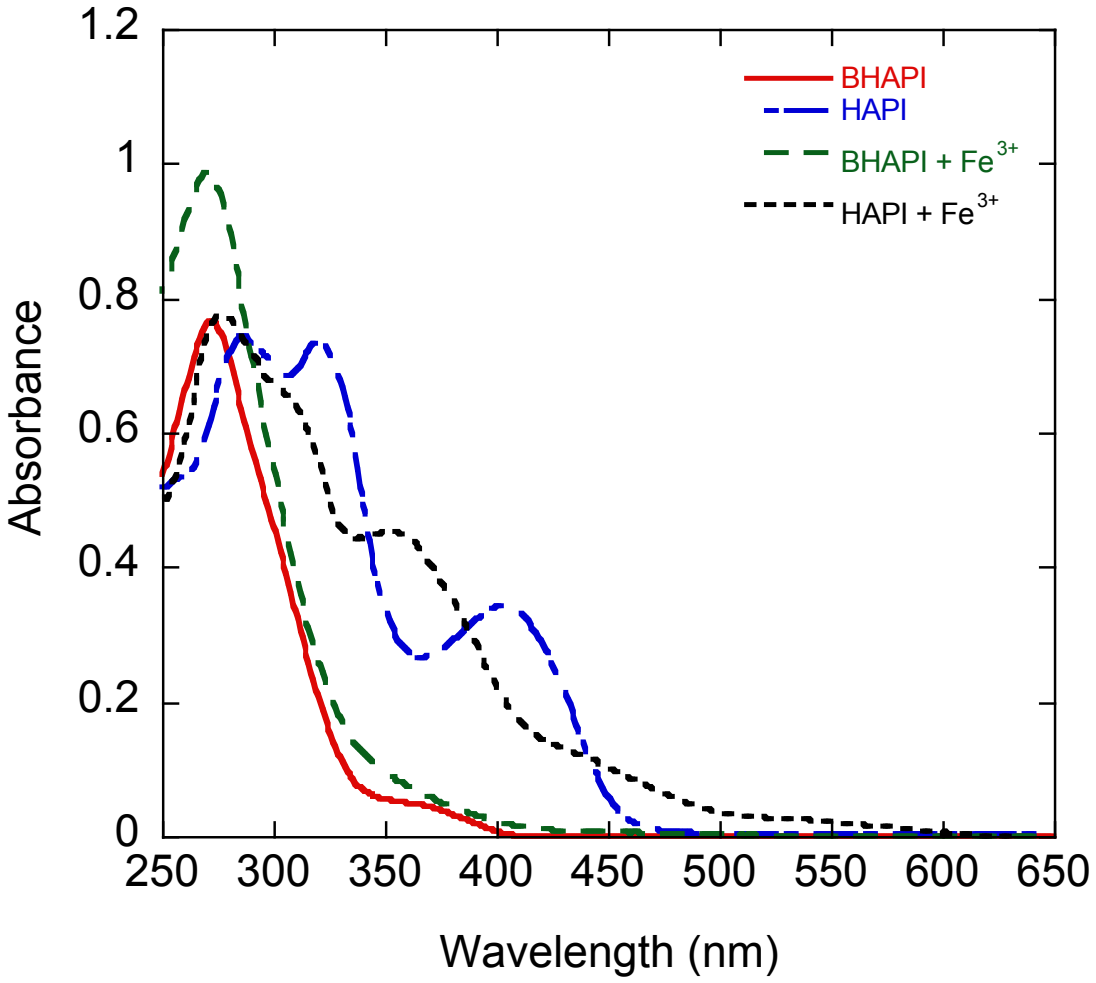

SI Fig. 10 UV-Vis spectra for interaction of BHAPI and HAPI (85 μM) with Fe^{3+} (85 μM) in PBS at pH 7.4.

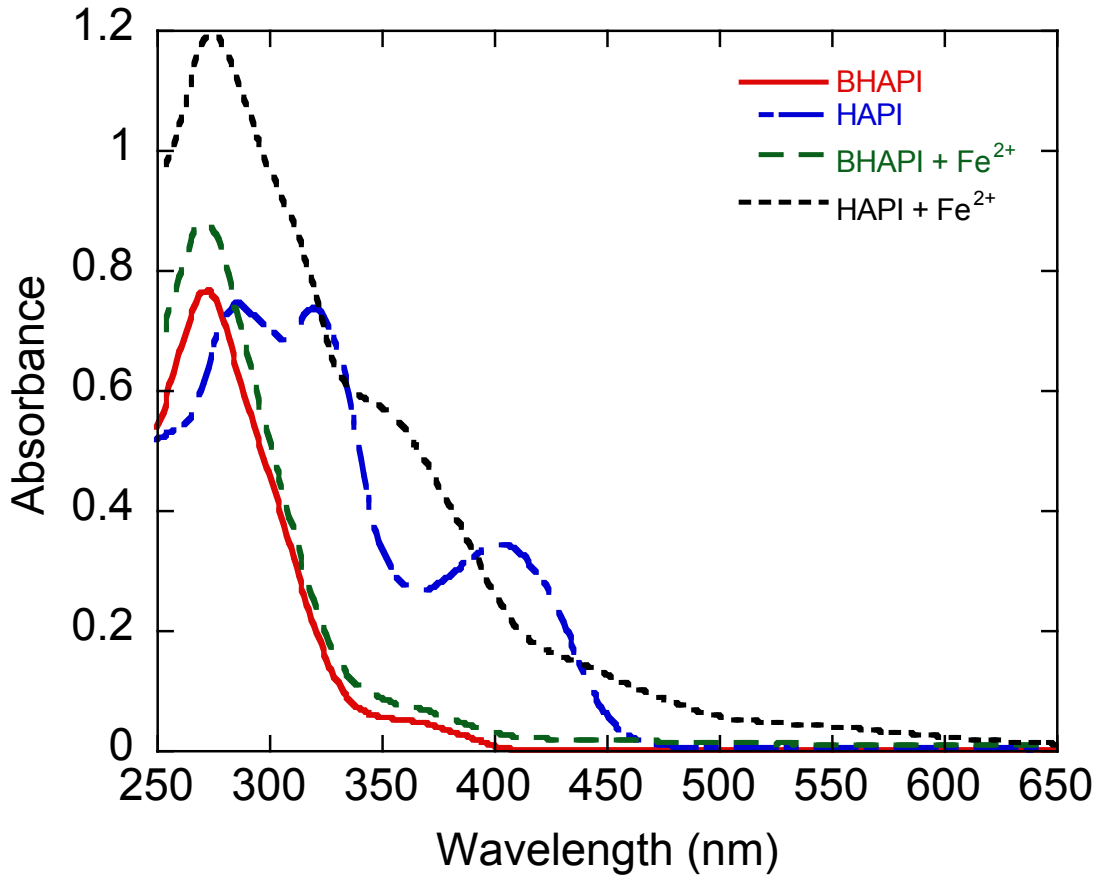

SI Fig. 11 UV-Vis spectra of BHAPI and HAPI (85 μM) in the absence and presence of one equivalent of Fe^{2+} in PBS at pH 7.4. The similarity in the spectra of HAPI after addition of either Fe^{2+} (dashed line above) or Fe^{3+} (main text Figure 7) suggests that HAPI facilitates oxidation to Fe^{3+}.

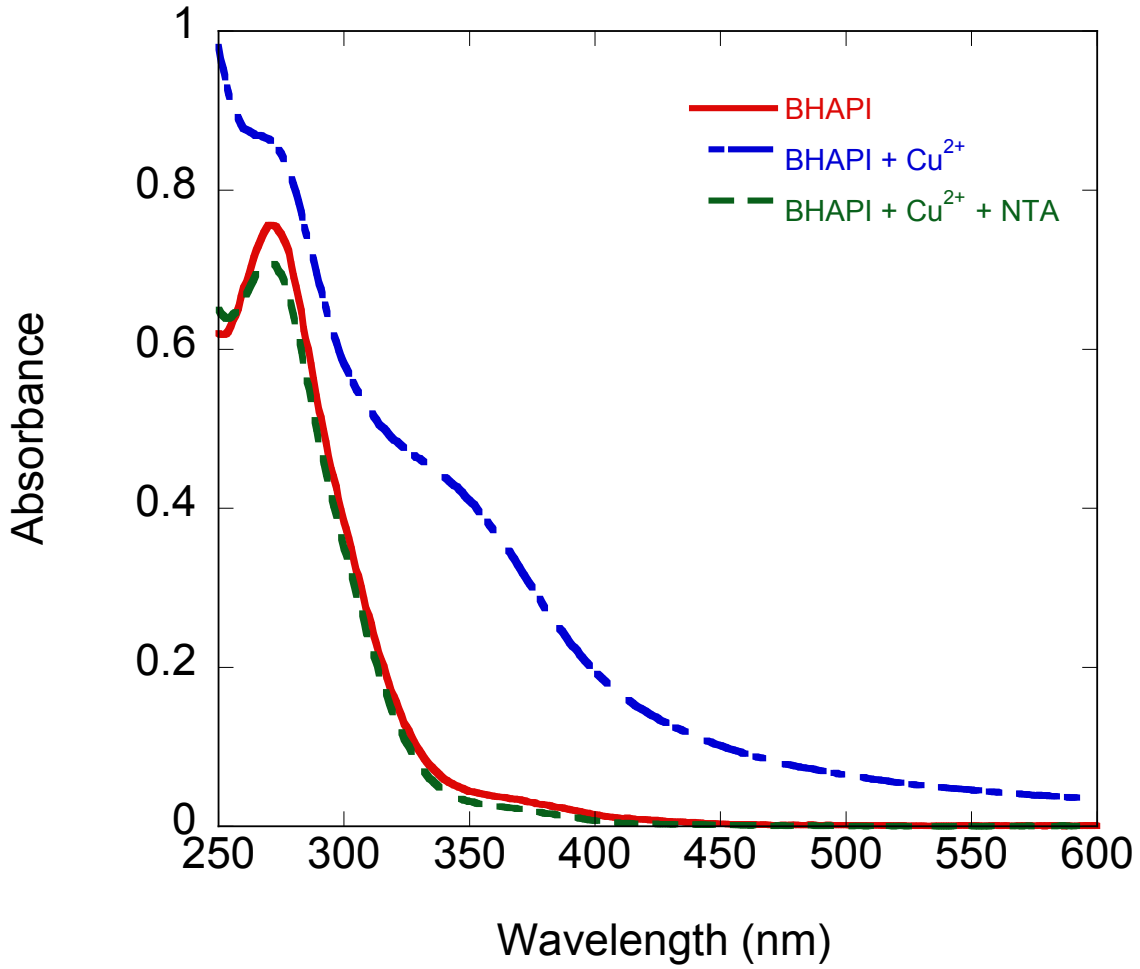

SI Fig. 12 UV-Vis spectra showing interaction of BHAPI (85 μM) with Cu^{2+} ion (85 μM) and the effect of NTA (85 μM) in PBS at pH 7.4.

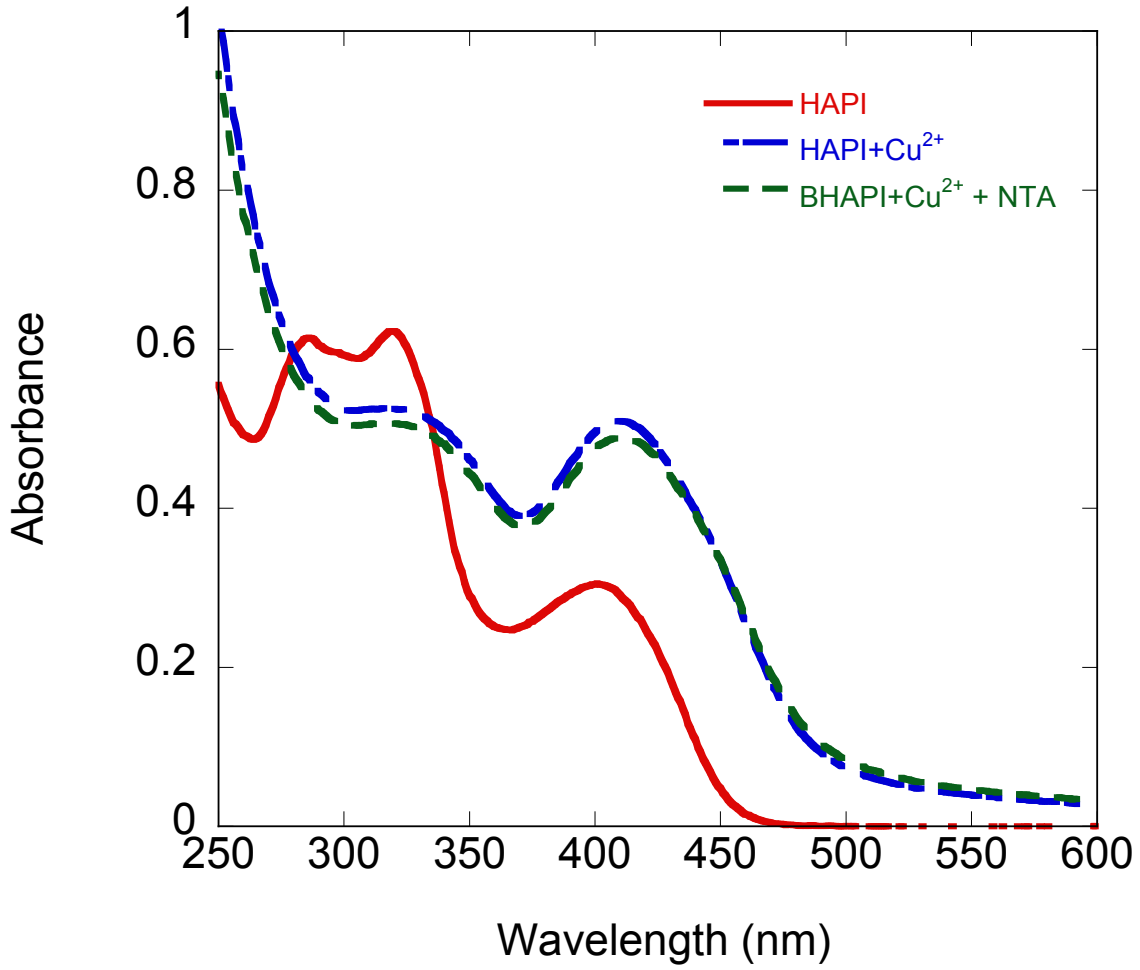

SI Fig. 13 UV-Vis spectra showing interaction of HAPI (85 μM) with Cu^{2+} ion (85 μM) and the effect of NTA (85 μM) in PBS at pH 7.4.

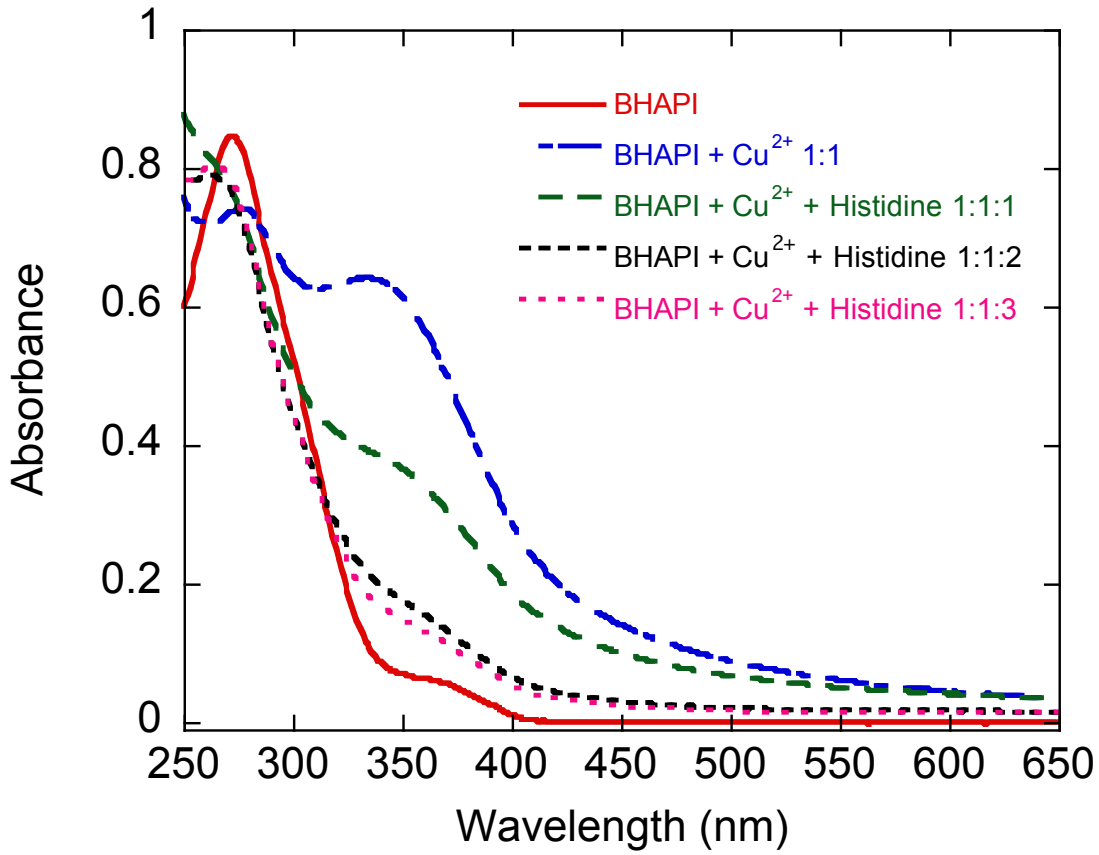

SI Fig. 14 UV-Vis spectra showing interaction of BHAPI (85 μM) with Cu^{2+} (85 μM) and the effect of added histidine in PBS at pH 7.4.

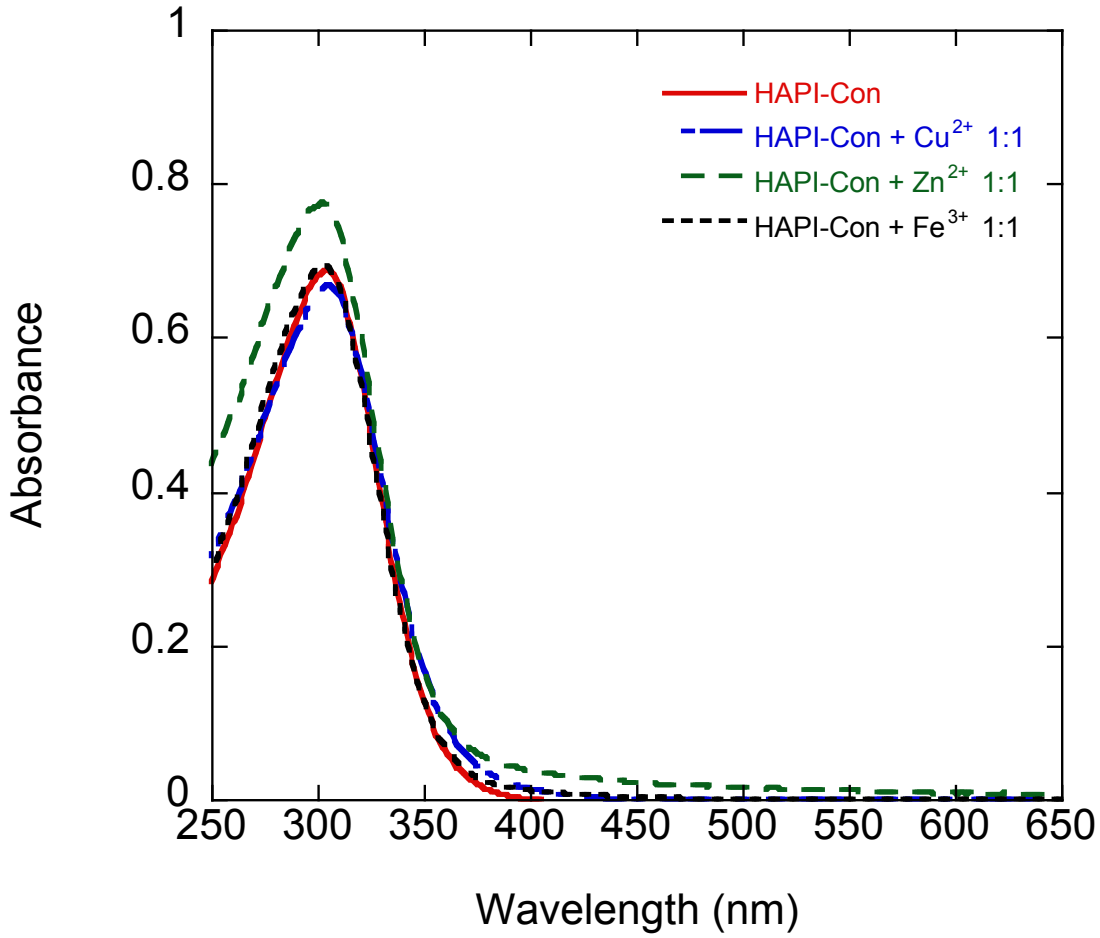

SI Fig. 15 UV-Vis spectra of HAPI-CON (85 μM) interaction with metal ions (85 μM) in PBS at pH 7.4

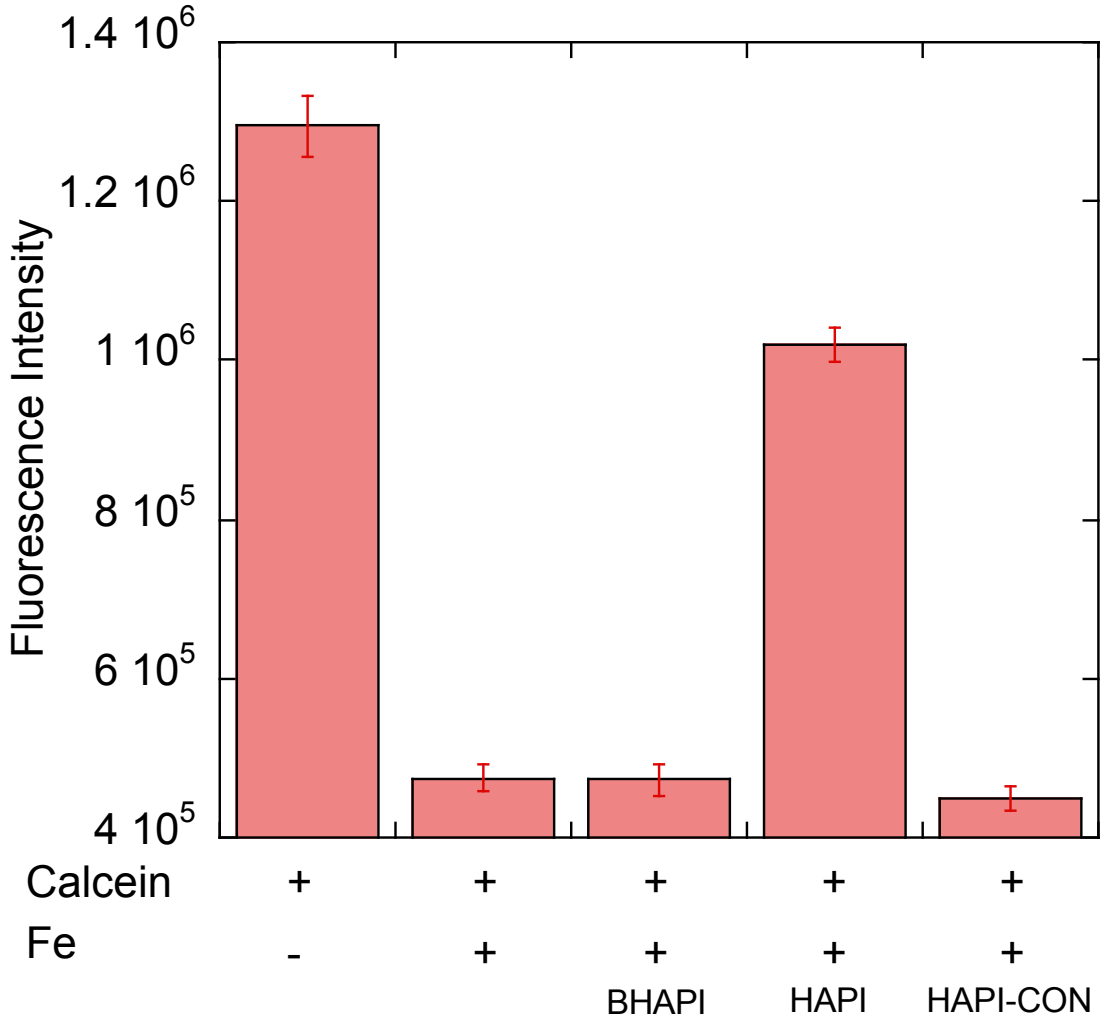

SI Fig. 16 Graph of calcein fluorescence (2 μM, PBS) quenching by iron (ferric ammonium citrate, 2 μM) and recovery by BHAPI, HAPI and HAPI-CON (4 μM).

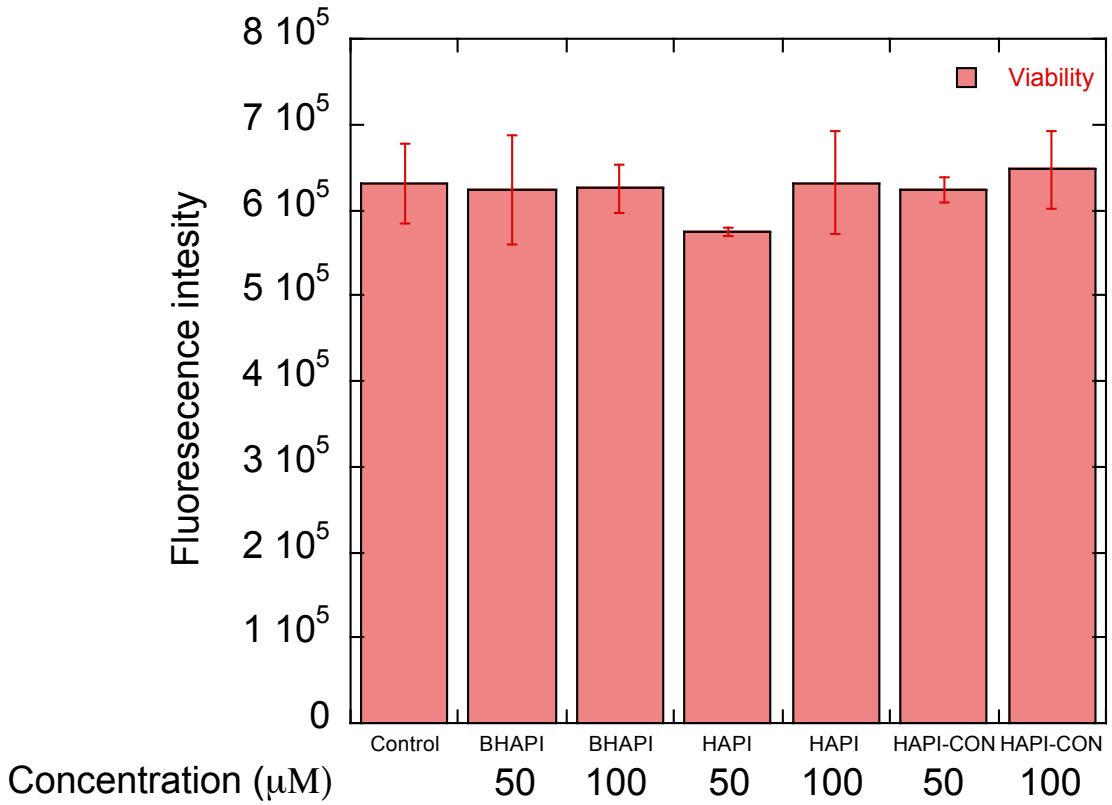

SI Fig. 17 Graph of cell viability for ARPE cells treated by BHAPI, HAPI, and HAPI-CON

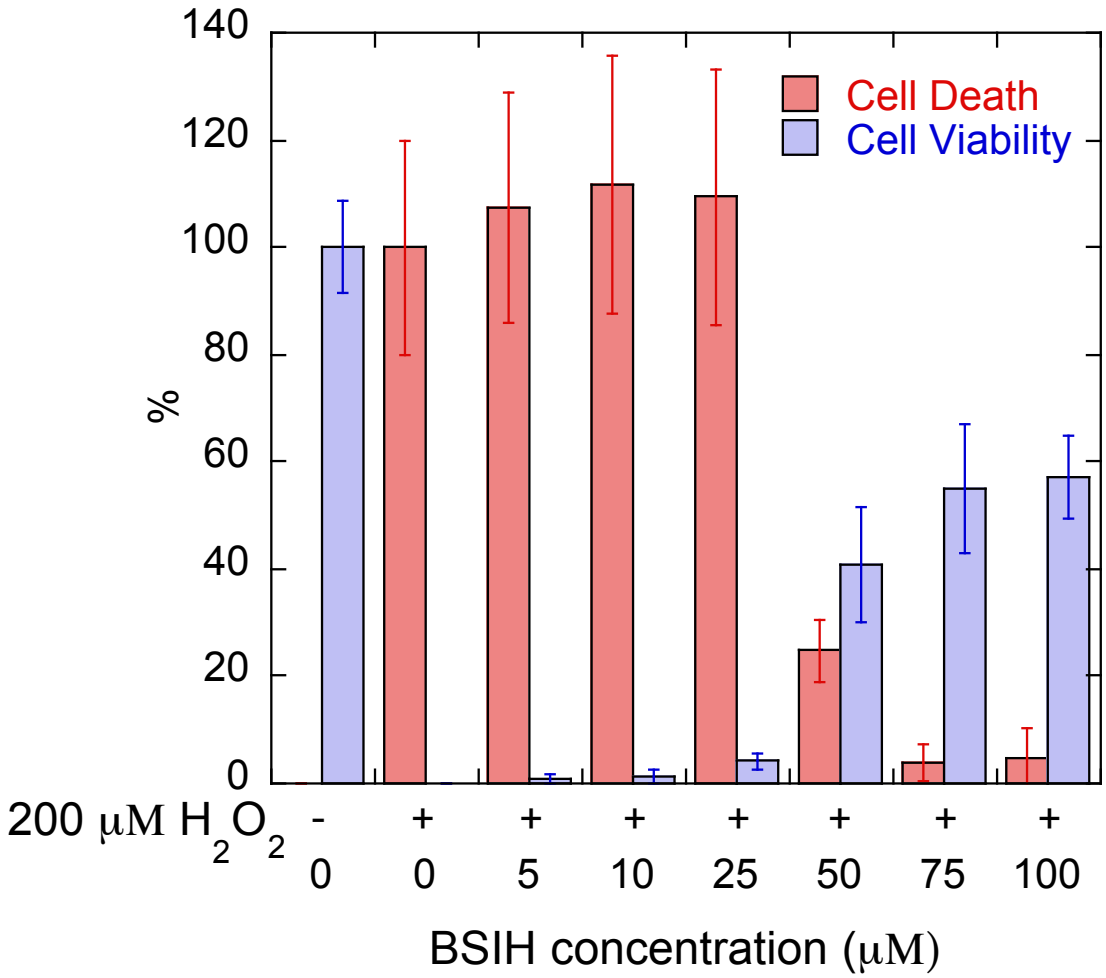

SI Fig. 18 Graph of cell viability of ARPE cells treated with H_2O_2 (200 μM) and protected by BSIH

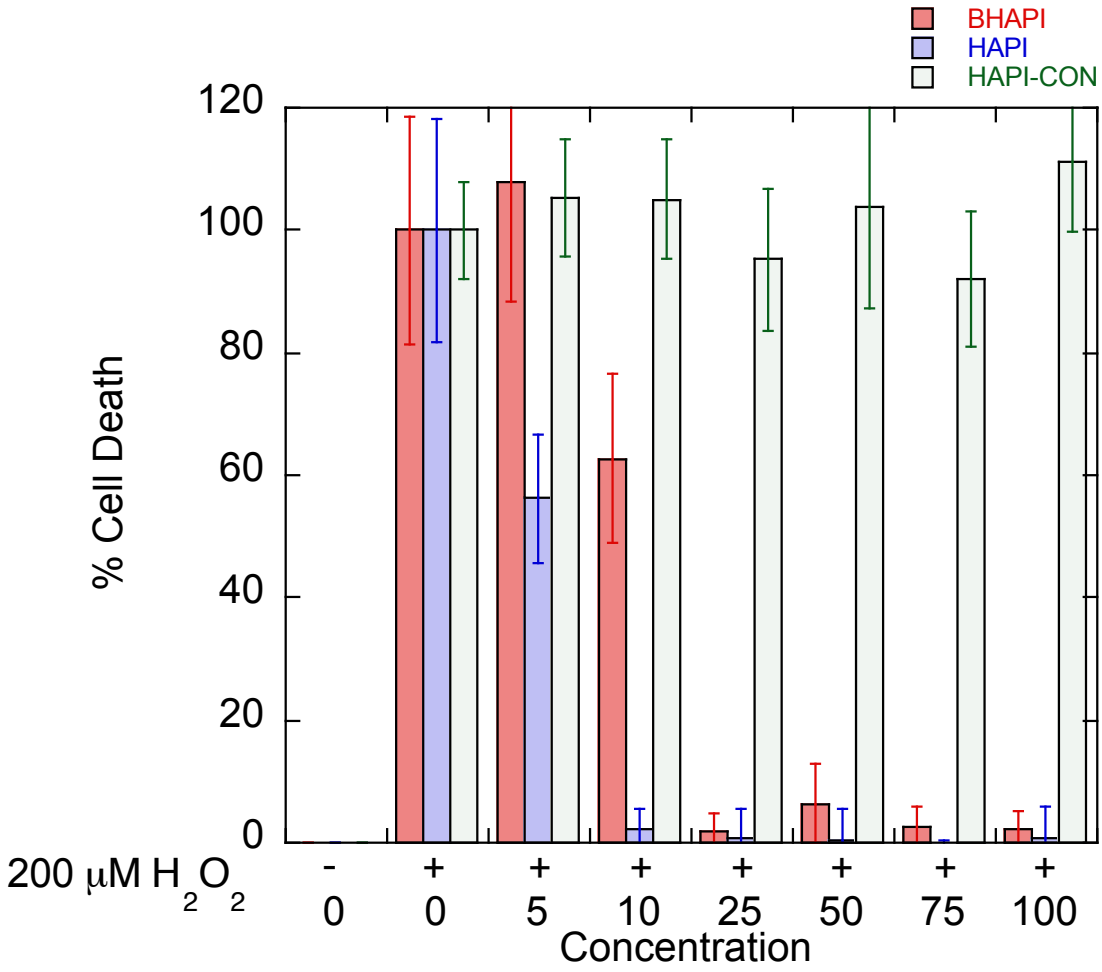

SI Fig. 19 Graph of cell death of ARPE cells treated with H_2O_2 (200 μM) and protected by BHAPI, HAPI, and HAPI-CON

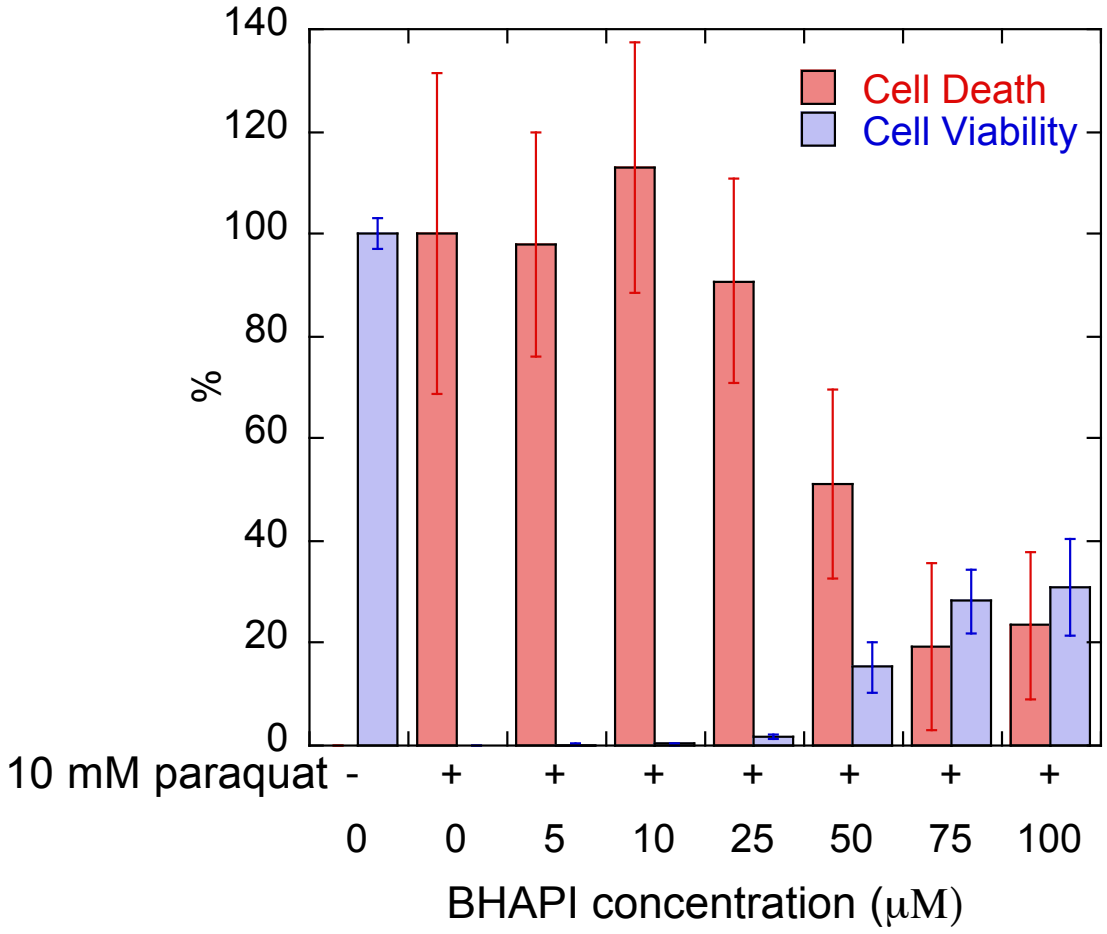

SI Fig. 20 Graph of protection of ARPE cells by BHAPI from paraquat (10 mM) exposure over 72 h.

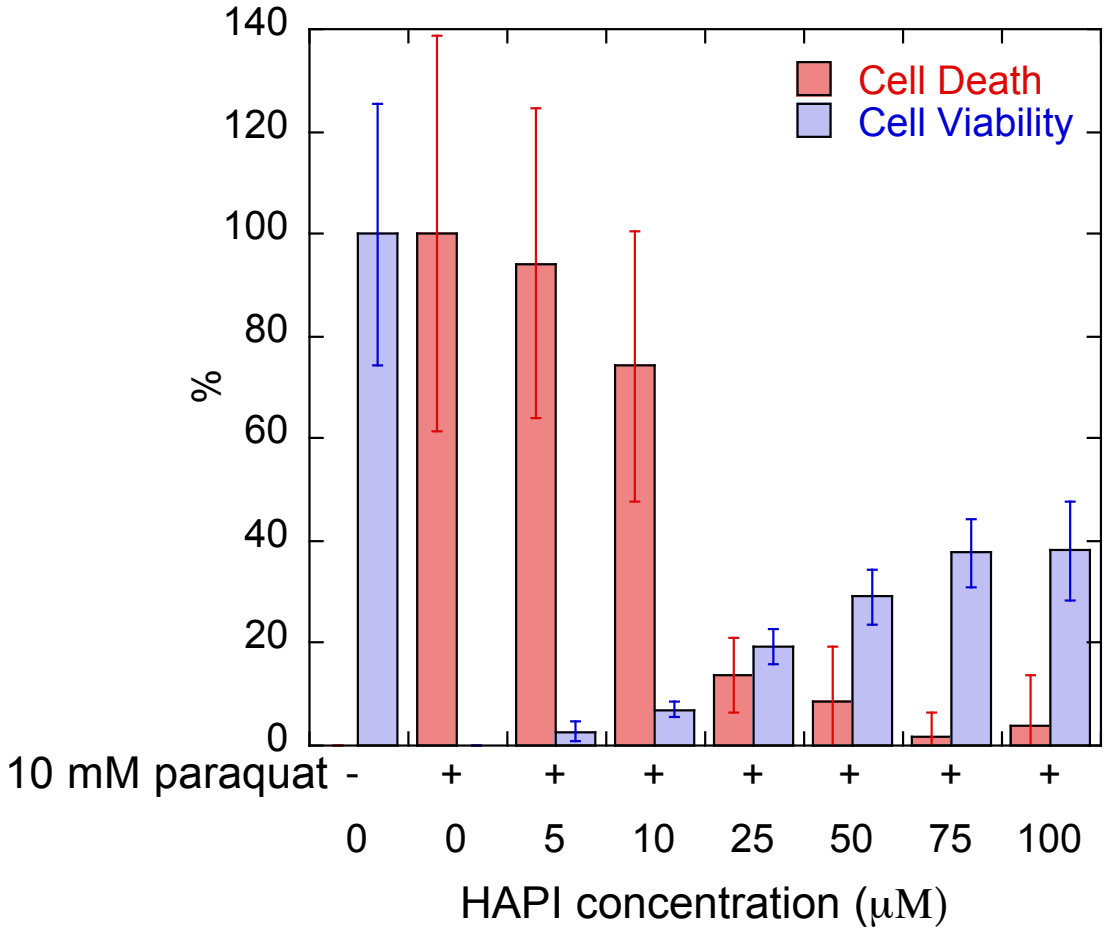

SI Fig. 21 Graph of protection of ARPE cells by HAPI from paraquat (10 mM) exposure over 72 h

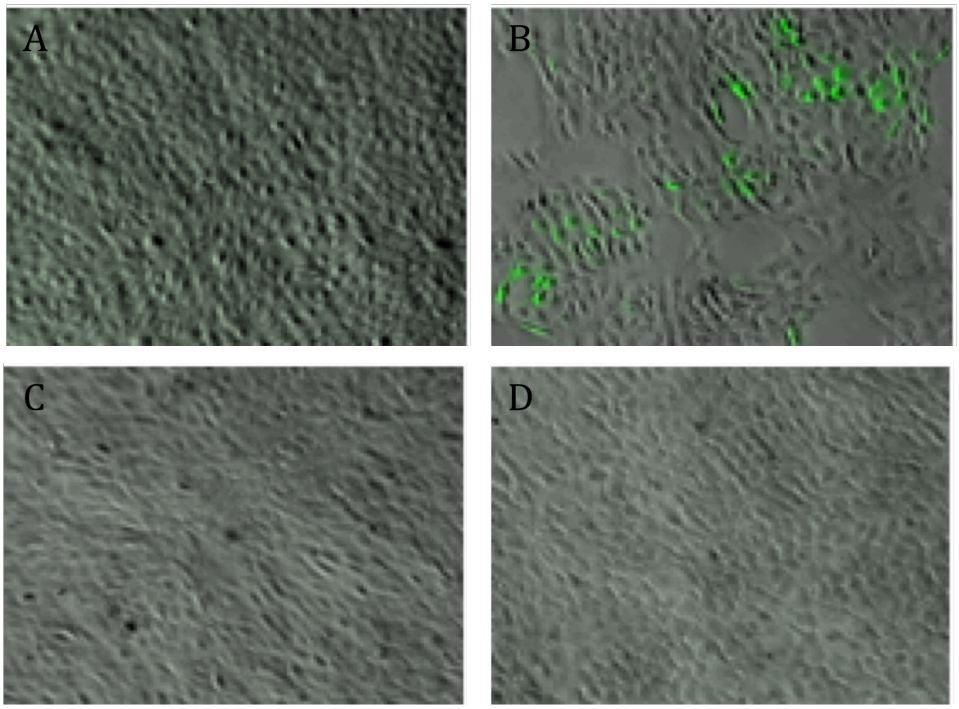

SI Fig. 22 Fluorescence images of cells labeled with dichlorodifluorofluorescein diacetate: (a) untreated cells, (b) cells treated with 10 mM paraquat, (c) cells treated with paraquat and 100 μM BHAPI, and (c) cells treated with paraquat and 100 μM HAPI. Fluorescence images are overlaid on brightfield view.